Multi-peak-spectra generation with Cherenkov radiation in a non-uniform single mode fiber

F. R. Arteaga-Sierra,[1,*] **C. Milián,**[2,5] **I. Torres-Gómez,**[1] **M. Torres-Cisneros,**[3] **A. Ferrando,**[4] **and A. Dávila** [1]

[1]*Centro de Investigaciones en Óptica, A.C., León Gto. 37150, Mexico*
[2]*Instituto de Instrumentación para Imagen Molecular (I3M), InterTech, Universidad Politécnica de Valencia, Camino de Vera S/N 46022, Valencia, Spain*
[3]*Optoelectronics Group, Electronics Department, FIMEE University of de Guanajuato, Salamanca Gto. 36730, Mexico*
[4]*Departament d'Òptica, Universitat de València, Burjassot (València). 46100, Spain*
[5]*Current address: Centre de Physique Théorique, École Polytechnique, CNRS, F-91128 Palaiseau, France*
[*]*arteaga@cio.mx*

Abstract: We propose, by means of numerical simulations, a simple method to design a non-uniform standard single mode fiber to generate spectral broadening in the form of "ad-hoc" chosen peaks from dispersive waves. The controlled multi-peak generation is possible by an on/off switch of Cherenkov radiation, achieved by tailoring the fiber dispersion when decreasing the cladding diameter by segments. The interplay between the fiber dispersion and the soliton self-frequency shift results in discrete peaks of efficiently emitted Cherenkov radiation from low order solitons, despite the small amount of energy contained in a pulse. These spectra are useful for applications that demand low power bell-shaped pulses at specific carrier wavelengths.

OCIS codes: (190.4370) Nonlinear optics; (060.5530) Pulse propagation and temporal solitons.

References and links

1. J. M. Dudley, G. Genty, and S. Coen, "Supercontinuum generation in photonic cristal fibers," Rev. Mod. Phys. **78**, 1135–1184 (2006).
2. V. Skryabin, and A. V. Gorbach, "Colloquium: Looking at a soliton through the prism of optical supercontinuum," Rev. Mod. Phys. **82**, 1287–1299 (2010).
3. W. H. Reeves, D. V. Skryabin, F. Biancalana, J. C. Knight, P. St. J. Russell, F. G. Omenetto, A. Efimov, and A. J. Taylor, "Transformation and control of ultra-short pulses in dispersion-engineered photonic crystal fibres," Nature **424**, 511–515 (2003).
4. P. Russell, "Photonic crystal fibers," Science **299**, 358–362 (2003).
5. J. C. Knight, "Photonic crystal fibres," Nature **424**, 847–851 (2003).
6. W. J. Wadsworth, A. Ortigosa-Blanch, J. C. Knight, T. A. Birks, T.-P. Martin Man, and P. St. J. Russell, "Supercontinuum generation in photonic crystal fibers and optical fiber tapers: a novel light source," J. Opt. Soc. Am. B **19**, 2148–2155 (2002).
7. T. A. Birks, W. J. Wadsworth, and P. St. J. Russell, "Supercontinuum generation in tapered fibers," Opt. Lett. **25**, 1415–1417 (2000).
8. S. T. Sørensen, U. Moller, C. Larsen, P. M. Moselund, C. Jakobsen, J. Johansen, T. V. Andersen, C. L. Thomsen, and O. Bang, "Deep-blue supercontinnum sources with optimum taper profiles - verification of GAM," Opt. Express. **20**, 10635–10645 (2012).

#202318 - $15.00 USD Received 2 Dec 2013; accepted 15 Jan 2014; published 28 Jan 2014

9. A. Kudlinski, M. Lelek, B. Barviau, L. Audry, and A. Mussot, "Efficient blue conversion from a 1064 nm microchip laser in long photonic crystal fiber tapers for fluorescence microscopy," Opt. Express **18**, 16640–16645 (2010).
10. A. C. Judge, O. Bang, B. J. Eggleton, B. T. Kuhlmey, E. C. Mägi, R. Pant, and C. Martijn de Sterke, "Optimization of the soliton self-frequency shift in a tapered photonic crystal fiber," J. Opt. Soc. Am. B **26**, 2064–2071 (2009).
11. C. Cheng, Y. Wang, Y. Ou, and Q. Iv, "Enhanced red-shifted radiation by pulse trapping in photonic crystal fibers with two zero-dispersion wavelengths," Opt. Laser Technol. **44**, 954–959 (2012).
12. A. V. Gorbach and D. V. Skryabin, "Light trapping in gravity-like potentials and expansion of supercontinuum spectra in photonic-crystal fibres," Nat. Photonics **1**, 653–657 (2007).
13. G. Moltó, M. Arevalillo-Herráez, C. Milián, M. Zacarés, V. Hernández, and A. Ferrando, "Optimization of supercontinuum spectrum using genetic algorithms on service-oriented grids," in *Proceedings of the 3rd Iberian Grid Infrastructure Conference* (IberGrid, 2009), pp. 137–147.
14. A. Ferrando, C. Milián, N. González, G. Moltó, P. Loza, M. Arevalillo-Herráez, M. Zacarés, I. Torres-Gómez, and V. Hernández, "Designing supercontinuum spectra using Grid technology," Proc. SPIE **7839**, 78390W (2010).
15. S. A. Dekker, A. C. Judge, R. Pant, I. Gris-Sánchez, J. C. Knight, C. Martjn de Sterke, and B. J. Eggleton, "Highly-efficient, octave spanning soliton self-frequency shift using a specialized photonic crystal fiber with low OH loss," Opt. Express **19**, 17766–17773 (2011).
16. N. Akhmediev and M, Karlsson, "Cherenkov radiation emitted by solitons in optical fibers," Phys. Rev. A **51**, 2602–2607 (1995).
17. C. Milián, D. V. Skryabin, and A. Ferrando, "Continuum generation by dark solitons," Opt. Lett. **34**, 2096–2098 (2009).
18. R. Zhang, X. Zhang, D. Meiser, and H. Giessen, "Mode and group velocity dispersion evolution in the tapered region of a single-mode tapered fiber," Opt. Express **12**, 5840–5849 (2004).
19. C. M. B. Cordeiro, W. J. Wadsworth, T. A. Birks, and P. St. J. Russell, "Engineering the dispersion of tapered fibers for supercontinuum generation with a 1064 nm pump laser," Opt. Lett. **30**, 1980–1982 (2005).
20. F. Biancalana, D. V. Skryabin, and A. V. Yulin, "Theory of the soliton self-frequency shift compensation by the resonant radiation in photonic crystal fibers," Phys. Rev. E **70**, 016615 (2004).
21. J. C. Travers, J. M. Stone, A. B. Rulkov, B. A. Cumberland, A. K. George, S. V. Popov, J. C. Knight, and J. R. Taylor, "Optical pulse compression in dispersion decreasing photonic crystal fiber," Opt.Express **15**, 13203–13211 (2007).
22. J. C. Travers and J. R. Taylor, "Soliton trapping of dispersive waves in tapered optical fibers," Opt. Lett. **34**, 115–117 (2009).
23. S. Pricking and H. Giessen, "Tailoring the soliton and supercontinuum dynamics by engineering the profile of tapered fibers," Opt. Express **18**, 20151–20163 (2010).
24. C. Milián, A. Ferrando, and D. V. Skryabin, "Polychromatic Cherenkov radiation and supercontinuum in tapered optical fibers," J. Opt. Soc. Am. B **29**, 589–593 (2012).
25. R. Zhang, J. Teipel, X. Zhang, D. Nau, and H. Giessen, "Group velocity dispersion of tapered fibers immersed in different liquids," Opt. Express **12**, 1700–1707 (2004).
26. H. J. Kbashi, "Fabrication of submicron-diameter and taper fibers using chemical etching," J. Mater. Sci. Technol. **28**, 308–312 (2012).
27. P. Cimalla, J. Walther, M. Mehner, M. Cuevas, and E. Koch, "Simultaneous dual-band optical coherence tomography in the spectral domain for high resolution in vivo imaging," Opt. Express **17**, 19486–19500 (2009).
28. J. G. Fujimoto, C. Pitris, S. A. Boppart, and M. E, Brezinski, "Optical coherence tomography: An emerging technology for biomedical imaging and optical biopsy," Neoplasia **2**, 9–25 (2000).
29. E. Lareau, F. Lesage, P. Pouliot, D. Nguyen, J. Le Lan, and M. Sawan, "Multichannel wearable system dedicated for simultaneous electroencephalography/near-infrared spectroscopy real-time data acquisitions," J. Biomed. Opt. **16**, 096014 (2011).
30. A. M. Smith, M. C. Mancini, and S. Nie, "Bioimaging: Second window for in vivo imaging," Nat. Nanotechnol. **4**, 710–711 (2009).
31. Q. Cao, N. G. Zhegalova, S. T. Wang, W. J. Akers, and M. Y. Berezin, "Multispectral imaging in the extended near-infrared window based on endogenous chromophores," J. Biomed. Opt. **18**, 101318 (2013).
32. J. M. Huntley, T. Widjanarko, and P. D. Ruiz, "Hyperspectral interferometry for single-shot absolute measurement of two-dimensional optical path distributions," Meas. Sci. Technol. **21**, 075304 (2010).
33. G. P. Agrawal, *Nonlinear Fiber Optics*, 4th ed. (Academic, 2007).
34. S. Afshar V., W. Q. Zhang, H. Ebendorff-Heidepriem, and T. M. Monro, "Small core optical waveguides are more nonlinear than expected: experimental confirmation," Opt. Lett. **34**, 3577–3579 (2009).
35. C. Milián and D. V. Skryabin, "Nonlinear switching in arrays of semiconductor on metal photonic wires," Appl. Phys. Lett. **98**, 111104 (2011).
36. www.optiwave.com.
37. D. V. Skryabin and A. V. Yulin "Theory of generation of new frequencies by mixing of solitons and dispersive waves in optical fibers," Phys. Rev. E **72**, 016619 (2005).
38. S. Roy, S. K. Bhadra, and G. P. Agrawal, "Dispersive wave generation in supercontinuum process inside nonlinear

#202318 - $15.00 USD Received 2 Dec 2013; accepted 15 Jan 2014; published 28 Jan 2014

microstructured fibre," Curr. Sci. **100**, 321–342 (2011).
39. J. P. Gordon, "Theory of the soliton self-frequency shift," Opt. Lett. **11**, 662–664 (1986).
40. A. V. Gorbach and D. V. Skryabin, "Soliton self-frequency shift, non-solitonic radiation and self-induced transparency in air-core fibers," Opt. Express **16**, 4858–4865 (2008).
41. A. V. Gorbach and D. V. Skryabin, "Theory of radiation trapping by the accelerating solitons in optical fibers," Phys. Rev. A **76**, 053803 (2007).
42. B. Metzger, A. Steinmann, F. Hoos, S. Pricking, and H. Giessen, "Compact laser source for high-power white-light and widely tunable sub 65 fs laser pulses," Opt. Lett. **35**, 3961–3963 (2010).
43. J. N. Farmer and C. I. Miyake, "Method and apparatus for optical coherence tomography with a multispectral laser source," U.S. Patent 6,538,817 filed October 17, 2000, and issued March 25, 2003.
44. J. M. Huntley, P. D. Ruiz, and T. Widjanarko, "Apparatus for the absolute measurement of two dimensional optical path distributions using interferometry," U.S. Patent 2,011,010,092 filed July 20, 2010, and issued July 12, 2012.
45. N. L. Everdell, I. B. Styles, A. Calcagni, J. Gibson, J. Hebden, and E. Claridge, "Multispectral imaging of the ocular fundus using light emitting diode illumination," Rev. Sci. Instrum. **81**, 093706 (2010).

1. Introduction

To fully exploit the nonlinear dynamics associated to Supercontinuum (SC) generation in optical fibers (see Refs. [1, 2] for reviews on the topic) it is customary to use photonic crystal fibers (PCFs), since they provide a versatile platform to accurately tune the linear and nonlinear dispersions governing the propagation of optical pulses [3–5]. However, other simpler and cheaper fiber designs can also yield wide spectra and provide certain control on the pulse propagation dynamics [6, 7], which may suffice for many applications. Nowadays, one of the aspects in SC generation receiving substantial interest is the management of the spectral output to obtain blue and infrared (IR) extended spectra [8–11], both effects associated to the red-shifting Raman solitons with trapped dispersive waves (DWs) [12]. Another important attribute to control in less broad spectra is the localization of spectral power in bands centered at specific target wavelengths, consisting on either dispersive waves [13, 14] or Raman solitons in the IR [15]. In the former case, the Cherenkov or dispersive radiation, emitted by solitons under the right phase matching conditions [16], is used as a suitable spectral peak generator. Although multi-peak Cherenkov spectra are automatically generated in both normal and anomalous group velocity dispersion (GVD) regions in the context of SC generation with bright [1, 2] and dark [17] solitons, these methods lack in general of control on the individual carrier wavelengths of the Cherenkov DWs.

In this work, we propose a method to design a non-uniform fiber to obtain discrete spectral peaks from the DWs emitted by solitonic pulses by an on/off switch of Cherenkov radiation. This cheap method consists in splicing few pieces of standard telecom single mode fiber (SMF) with different cladding diameters, which can be achieved easily via post processing techniques that provide control on the GVD [18, 19]. For the pump, we consider the short pulses provided by a standard IR micro-chip laser. Switching on and off the Cherenkov radiation is achieved by adjusting the spectral distance between the zero GVD wavelength, λ_{zGVD}, and the Raman shifting soliton carrier, λ_s, which dramatically controls the radiation efficiency [20]. Several Cherenkov peaks emitted from a single soliton are possible because of the interplay between Raman and recoil induced red-shift, and the λ_{zGVD} management. Such management has proven very useful for manipulating the soliton propagation dynamics for, e.g, pulse compression [21], trapping of the Cherenkov radiation in the absence of Raman effect [22], controlling DW generation in the SC dynamics [23], and generation of a powerful continuum of Cherenkov radiation shed by a single soliton pulse [24]. Practical and low cost methods to tailor the λ_{zGVD} in fibers consist in immersing them in different liquids [25] or reducing their cladding diameter by using chemical etching methods that achieve submicron-diameters [26]. We have used the latter idea, for illustrative purposes, and have computed the linear dispersions and nonlinear coefficients

#202318 - $15.00 USD Received 2 Dec 2013; accepted 15 Jan 2014; published 28 Jan 2014

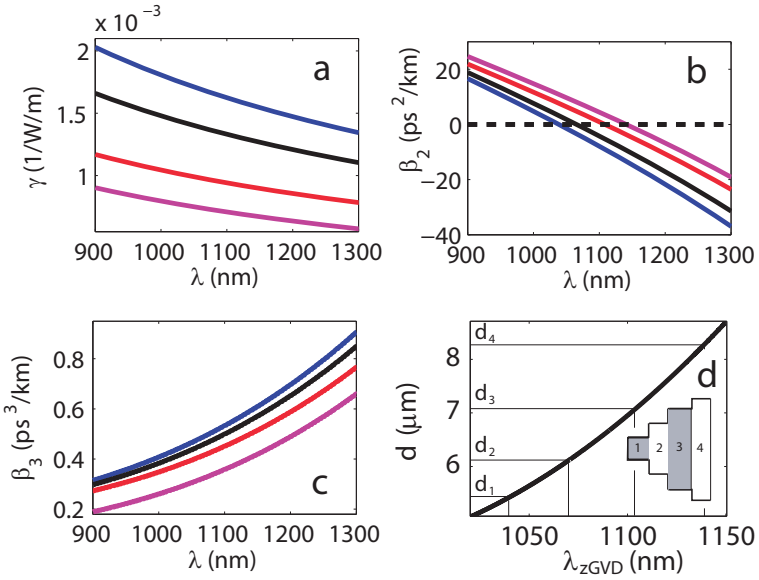

Fig. 1. (a) Nonlinear coefficient, (b) GVD, and (c) third order dispersion (TOD) for the different cladding diameters: $d = 5.4$ (blue), 6.1 (black), 7.1 (red) and 8.3 μm (magenta). The corresponding values of λ_{zGVD} are: 1035, 1070, 1105, and 1140 nm (see b). (d) Dependence of the cladding diameter, d, on λ_{zGVD}. Inset shows a schematic side view of the non-uniform fiber, in which light propagation occurs from left to right [see Fig. 3(a)]. Diameters, d, and lengths, L, of the different regions are chosen as: $d_1 = 5.4$, $d_2 = 6.1$, $d_3 = 7.1$, $d_4 = 8.3$ μm; $L_1 = 35$, $L_2 = 40$, $L_3 = 55$, $L_4 = 90$ cm.

of several SMFs with different cladding diameters [see Fig. 1]. We envisage that this spectral peak generator will be useful for applications in areas such as optical coherence tomography (OCT) [27, 28], spectroscopy [29], multi-spectral imaging [30–32], and the applications where spectral peaks are required to carry few hundreds of Watts and to present Gaussian-like bell shapes.

2. Pulse-propagation in the non-uniform fiber

We simulate the propagation of fs-pulses with complex amplitude $A(z,T)$ by integrating numerically the generalized nonlinear Schrödinger equation (GNLSE) [33],

$$\frac{\partial A}{\partial z} = i\sum_{q\geq 2}\frac{\beta_q}{q!}[i\partial_T]^q A + i\gamma A\int_{-\infty}^{+\infty} R(T')|A(z,T-T')|^2 dT', \tag{1}$$

where z is the coordinate along propagation and $T \equiv t - \beta_1 z$ the co-moving time. This equation accounts for the linear dispersion through the coefficients $\beta_q \equiv d^q\beta(\omega)/d\omega^q|_{\omega=\omega_0}$ (up to $q = 10$) evaluated at the pump frequency $\omega_0 = 2\pi c/\lambda_0$ ($\lambda_0 = 1060$ nm) of the laser. Nonlinearity is included through the parameter γ and the response function $R(T) \equiv [1 - f_R]\delta(T) + f_R h_R(T)\Pi(T)$, where $f_R = 0.18$, h_R is the commonly used Raman response of silica [33], and $\delta(T)$, $\Pi(T)$ are the Dirac, Heaviside functions, respectively. The definition of the nonlinear parameter used here constitutes a good approximation for our large core fibers [see Fig. 1], and therefore we do not need to use the recently experimentally [34] and numerically [35] tested coefficients for sub-wavelength waveguides. The input pulses in our modeling are taken

#202318 - $15.00 USD Received 2 Dec 2013; accepted 15 Jan 2014; published 28 Jan 2014

as $A(z=0,T) \equiv \sqrt{P_0}\,\mathrm{sech}(T/\tau_0)$ with $P_0 \equiv P(z=0) = 10$ kW and intensity full width at half maximum (FWHM) $\tau_{FWHM} = 65$ fs ($\tau_0 \equiv \tau(z=0) \equiv \tau_{FWHM}/2\ln[1+\sqrt{2}] \approx 36.85$ fs). With these parameters, the soliton order, $N \equiv \tau[\gamma P/|\tilde{\beta}_2|]^{1/2}$, is kept below fission threshold, $1 \leq N < 2$, for the input conditions ($\tilde{\beta}_q \equiv \partial_\omega \beta(\omega)|_{\omega=\omega_s}$ are the instantaneous coefficients).

Figure 1 shows the nonlinear parameter, $\gamma(\lambda)$, and the lower order dispersion coefficients, $\beta_{2,3}(\lambda)$, for the different pieces of our SMF, with different cladding diameters, computed using Optiwave [36]. The key role played by the position of the λ_{zGVD} along propagation in the radiation switch requires to have a fine control of it. From our numerical data of dispersion in Fig. 1(b), it is possible to find a convenient fit to link it with the SMF cladding diameter, d [see Fig. 1(d)]:

$$d(\mu m) \cong 8.6434\times10^{-5}\lambda_{zGVD}^2(nm) - 1.5958\times10^{-1}\lambda_{zGVD}(nm) + 77.9036, \tag{2a}$$

$$\lambda_{zGVD}(z) \approx \lambda_s\left[1+\frac{\lambda_s}{12\pi c\delta_3\tau}\right]^{-1}, \tag{2b}$$

where $\delta_3 \equiv \tilde{\beta}_3/6\tau|\tilde{\beta}_2|$ is the z-dependent (through $\lambda_s(z)$, $\tau(z)$) normalized TOD coefficient (recall that $\tilde{\beta}_q \equiv \partial_\omega\beta(\omega)|_{\omega=\omega_s}$).

3. Generation of discrete Cherenkov spectra

Cherenkov radiation is emitted at a frequency $\omega_{Ch} = 2\pi c/\lambda_{Ch}$ for which the propagation constant of the linear waves, β_{Ch}, matches that of the soliton, β_s, so both propagate with the same phase velocity [37]. The matching condition $\beta_{Ch}(\lambda) \equiv \beta_s(\lambda)$ can be expressed approximately for small δ_3 by [38]

$$\lambda_{Ch}(\delta_3) \approx \left[\frac{1+4\delta_3^2(2N-1)^2}{4\pi\delta_3\tau c} + \frac{1}{\lambda_s}\right]^{-1}, \tag{3}$$

and may be visualized by plotting the soliton and radiation dispersion relations, $k_s = \gamma P/2$ and $k_{Ch} = \sum_{q\geq2}\tilde{\beta}_q(\omega-\omega_s)^q/q!$, versus wavelength [2], as shown in Fig. 2(a) for several stages of the propagation in the non-uniform fiber [see Fig. 3].

Figure 3 shows spectral and temporal evolution of an $N(z=0) \approx 1.7$ pulse along the non-uniform SMF consisting of four pieces [see Fig. 1(d)]. At the entrance of each of the four pieces the solitons emit blue shifted dispersive radiation during a very short propagation distance, before the recoil effect sharply red-shifts the solitons and frustrates the radiation emission [2]. After this first fast process, the only role played by the fiber segment with uniform cross section is that of decreasing the soliton frequency through the Raman induced soliton self-frequency shift (SSFS) [39]. This is however, together with the recoil effect, the mechanism we benefit from to tune the soliton wavelength. By tracking $\lambda_s(z)$ and $\tau(z)$ along propagation in a given segment of the SMF, we can efficiently generate a new Cherenkov spectral peak at a desired wavelength, λ_{zGVD} [red-shifted from the previous one, see Fig. 2], by splicing a new SMF segment with d given by combining the inverted version of Eq. (3),

$$\delta_3 \approx \frac{\pi c\tau\left[\frac{1}{\lambda_{Ch}}-\frac{1}{\lambda_s}\right] + \sqrt{\pi^2c^2\tau^2\left[\frac{1}{\lambda_{Ch}}-\frac{1}{\lambda_s}\right]^2 - [2N-1]^2}}{2[2N-1]^2}, \tag{4}$$

together with Eqs. (2a)–(2b). In obtaining Eq. (4) we restricted ourselves to the case $\delta_3 > 0$ (i.e., around the first zero GVD wavelength). Note that in our problem, the analytical method of

#202318 - $15.00 USD Received 2 Dec 2013; accepted 15 Jan 2014; published 28 Jan 2014

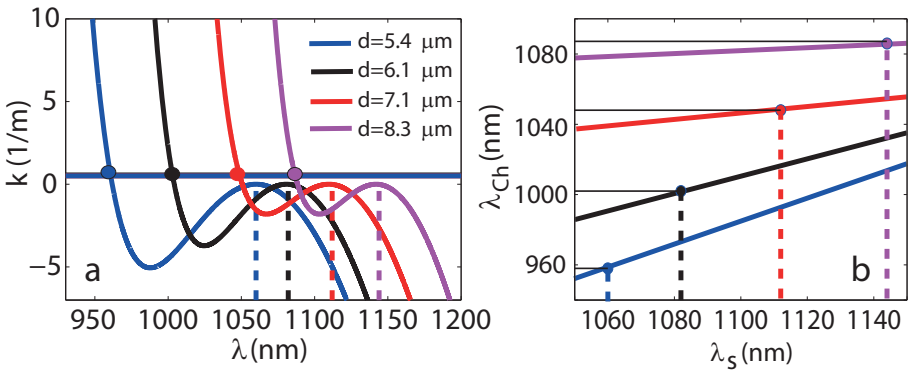

Fig. 2. (a) Phase matching between the fundamental soliton (straight line) and the DWs (curves), and (b) dependence of λ_{Ch} on λ_s in the decreasing cladding diameter SMF with $d_1 = 5.4$ (blue), $d_2 = 6.1$ (black), $d_3 = 7.1$ (red), and $d_4 = 8.3$ μm (magenta). Dots indicate the corresponding Cherenkov radiation wavelength, λ_{Ch}, and dashed lines mark the soliton central wavelength, λ_s. The four cases considered here correspond to the distances at which the soliton enters a new SMF segment [see Fig. 3(a)].

Ref. [39] can not be used to predict accurately the carrier frequency of the soliton after certain propagation distance because the radiation emission induces spectral recoil and (although less important) a drift in the soliton order, N [see Fig. 3(c)].

Despite the low initial value for the soliton order, $1 \leq N(z=0) < 2$, and the fact that it releases energy in the form of Cherenkov waves, the frequency conversion keeps being highly efficient due to the decrease in $|\beta_2(\lambda_s)|$ at the entrance of each of the new fiber segment, which keeps $N > 1$ [see Fig. 3(c)]. This defines the limiting factor of the device: N is kept > 1 because $|\beta_2(\lambda_s)|$ is decreased by moving the λ_{zGVD} closer and closer to λ_s, however this is valid as long as λ_{zGVD} does not fall within the soliton spectral width (e.g., within its spectral FWHM). At the beginning of the fourth segment, the drastic change of the λ_{zGVD} caused an increase of $N \sim 2.3$ and the subsequent fission into two fundamental solitons [see Fig 3(a)].

Because the short pulses we consider here ($\tau_0 < 50$ fs), the Raman gain induces an additional perturbation to solitons and they release strong radiation in the form Airy waves [40], which carrier frequency is in the anomalous GVD and slightly above than that of the soliton. In our non-uniform fiber the solitons can trap these waves [41], which may be used as additional spectral peaks since being trapped they maintain a localized shape in time domain. To show that the peaks generated here are localized in both time and spectrum, we plot in Fig. 4(a) the XFROG corresponding to the final stage of the propagation in Fig. 3 ($z = 2.1$m). Spectrogram is computed as $\Sigma(\omega, T) = |\int_{-\infty}^{\infty} A(T')g(T'-T)e^{-i\omega T'}dT'|$, the gate function is $g(\zeta) = \mathrm{sech}(\zeta/\tau_g)$ with $\tau_g = 30$ fs. If the tunneling of Airy waves through the soliton is not desired, it is possible to avoid it by elongating the third section of the fiber, thus keeping them separated in time domain from the Cherenkov radiation by the soliton. this is shown in the XFROG Fig. 4(b). Simultaneous temporal and spectral representation of light states can be experimentally measured with great resolution and quality [42], providing evidence of the right performance of the non-uniform fiber spectral peak generator.

The growing interest in building light sources for OCT has led to investigation of several methods to achieve multi-peak spectra [43–45]. In some of these approaches a specific laser source is required for each of the spectral peaks [43–45], and in others specific filters are applied to white light LED sources [45]. Therefore these methods have an independent control on the frequency of the bands which can be in principle largely detuned to each other, but they are,

#202318 - $15.00 USD Received 2 Dec 2013; accepted 15 Jan 2014; published 28 Jan 2014

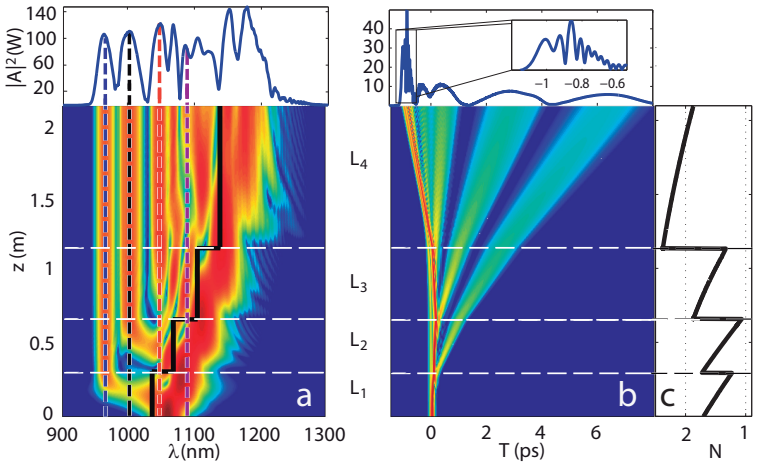

Fig. 3. (a) Spectral and (b) temporal evolution of an input pulse at $\lambda_0 = 1060$ nm with $P_0 = 10$ kW and a width of 65 fs (FWHM). The shifting λ_{zGVD} (initially at 1035 nm) is marked by the solid black line in (a) and the vertical dashed correspond to the λ_{Ch} predicted by Eq. (3): 958 (blue), 1002 (black), 1048 (red) and 1086 nm (magenta). (c) Evolution of the soliton order, N, for each fiber segment of length L_j. The value of N is approximately the same for both solitons resulting from fission by the end of the last segment, L_4 (both $N(z)$ lines overlap).

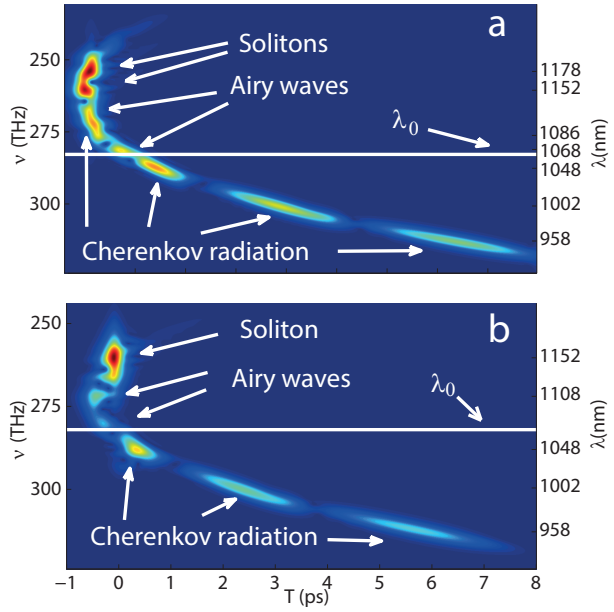

Fig. 4. XFROG traces, $\Sigma(\nu = \omega/2\pi, T)$, for the output field ($z = 2.1$ m) of (a) Fig. 3(a) and (b) Fig. 3(b). Horizontal white lines mark the pump.

#202318 - $15.00 USD Received 2 Dec 2013; accepted 15 Jan 2014; published 28 Jan 2014

on the other hand, dependent on many sources and relatively complex setups. The advantage presented by the method we propose in this paper is that only one light (Laser) source is needed to produce several localized spectral peaks with distributed power at the same time that they correspond to optical pulses with bell shaped profiles produced with cheap components.

4. Conclusions

We have presented a versatile method to obtain a multi-peak spectra exhibiting predefined discrete peaks arising from IR Cherenkov radiation emitted from bright solitons. This mechanism is based on an on/off switch made by splicing several pieces of uniform SMF and pumping with a micro-chip laser at 1060 nm. This is motivated by the wide interest that the second near IR window (950-1350 nm) presents for medical imaging. This device can be efficiently controlled by the adequate design of the GVD profiles of each fiber segment, being the zero dispersion wavelength, λ_{zGVD}, the key parameter to control. Our numerical results show the generation of three or four well defined peaks [see Figs. 3–4] when we launch a 65 fs/10 kW solitonic pulse in the non-uniform fiber consisting on four uniform sections, each of them with different cladding diameters [see Fig. 1]. These diameters can be selected in order to obtain highly efficient energy transfer between the soliton and the DWs at selected wavelengths. Additionally, strong remnants of Airy waves also grow in the spectrum which may constitute an interesting extra degree of freedom to control the spectral profile. Our analysis demonstrates that a single soliton ($N < 2$) is enough to efficiently generate several spectral peaks from dispersive waves. This method is versatile for applications requiring the simultaneous illumination with light containing multiple and specific wavelengths and can be implemented using off-the-shelf optic components such as a standard SMFs and common laser sources.

Acknowledgments

F.R.A.S. thanks the Consejo Nacional de Ciencia y Tecnología (CONACyT) grant. F.R.A.S. and I.T.G. acknowledge CONACyT for partial support, project: 106764 (CB-2008-1). Also, M.T.C. would like to thank for the partial funding provided to this work through the projects; DAIP-UG 01/12 and CONCyTEG GTO-2012-C03-195247. The work of A.F. was supported by the MINECO under Grant No. TEC2010-15327.

#202318 - $15.00 USD Received 2 Dec 2013; accepted 15 Jan 2014; published 28 Jan 2014